Electronic Supplementary Information

Tyndall-effect-based colorimetric assay with colloidal silver nanoparticles for quantitative point-of-care detection of creatinine using a laser pointer pen and a smartphone

Kaijing Yuan, Yao Sun, Fenchun Liang, Fenglan Pan, Miao Hu, Fei Hua, Yali Yuan,* Jinfang Nie,* Yun Zhang*

Guangxi Key Laboratory of Electrochemical and Magnetochemical Function Materials, College of Chemistry and Bioengineering, Guilin University of Technology, 12 Jiangan Road, Guilin 541004, P.R. China.

*Corresponding author.

E-mail addresses: zy@glut.edu.cn (Y. Zhang); Niejinfang@glut.edu.cn (J.-F. Nie); thankSIN2013@163.com (Y.-L. Yuan).

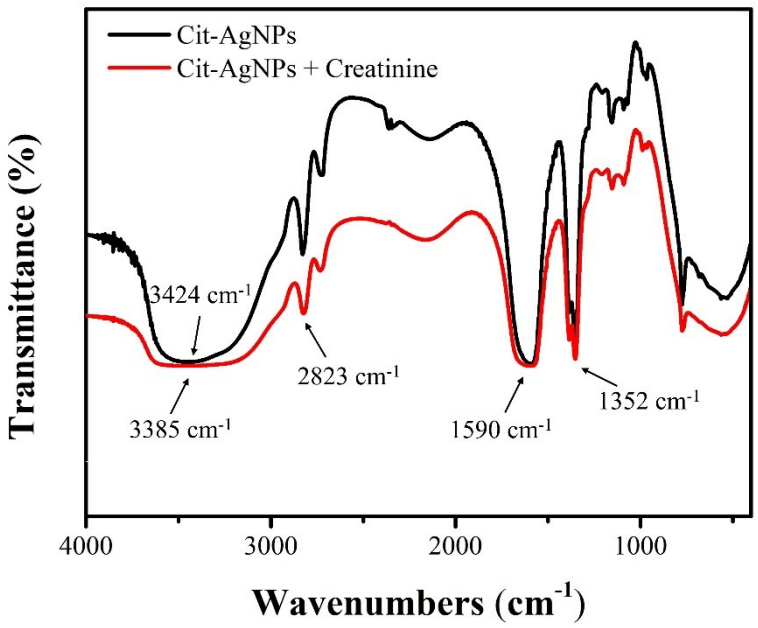

Fig. S1. FTIR spectra of Cit-AgNPs before (black line) and after (red line) the creatinine reaction. The creatinine molecules contain free NH_2, and their N-H stretching frequency appears between 3300-3500 cm^{-1}.[1] For the Cit-AgNPs, the peak variation around 3424 cm^{-1} can be attributed to the stretching vibration of O-H. The peak variation at 3385 cm^{-1} after the addition of creatinine to Cit-AgNPs is due to the overlapping stretching vibration of -N-H and O-H, where the stretching moves to higher frequencies. The peak becomes wider and smoother, which is attributed to the formation of hydrogen bonds between Cit-AgNPs and creatinine. The peak around 2823 cm^{-1} is the C-H stretching vibration, while the change in the peak around 1590 cm^{-1} is due to the C=O stretching of the carboxyl group and the -N-H bending vibration of the amino group, apparently, the absorption band appearing at 1352 cm^{-1} shows the C-H internal bending vibration of AgNPs.

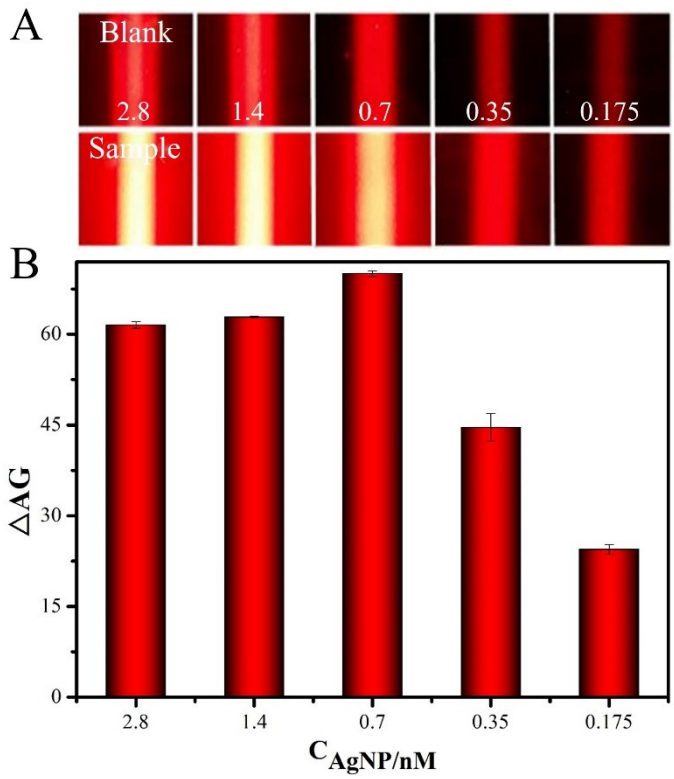

Fig. S2. (A) TE images obtained by mixing the blank group (i.e., water without analytes, top) and the experimental group (5 μM Creatinine, bottom) with AgNP solutions at different levels, respectively. The average grayscale change (ΔAG = $AG_{Creatinine}$ - AG_{blank}) of each TE response shown in (A) was provided in (B). Each error bar is the standard deviation of three repeated parallel experiments. The results suggest that 0.7 nM should be chosen as the optimal AgNP concentration as it produced the highest ΔAG value. Therefore, 0.7 nM AgNP was chosen as the optimal AgNP concentration for the next experiments.

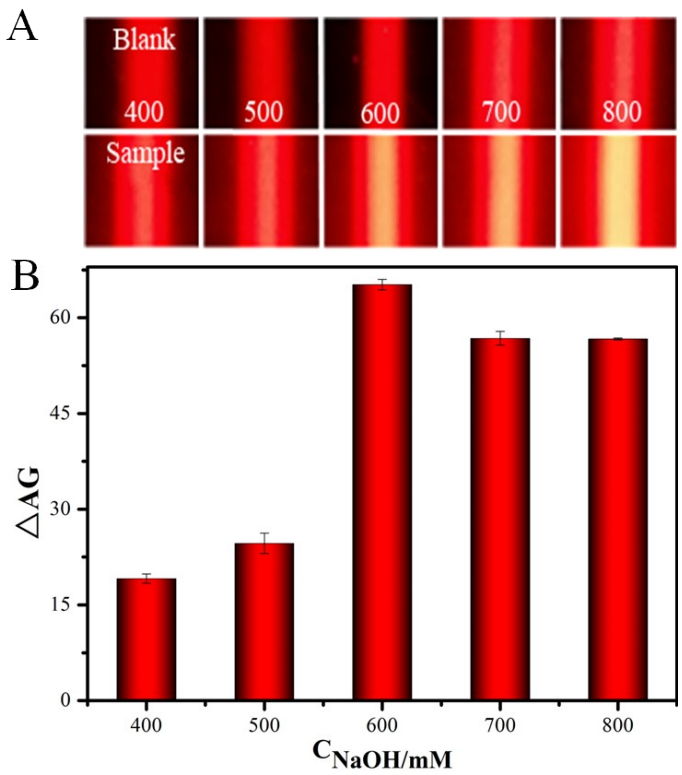

Fig. S3. (A) TE images obtained by mixing the blank group (i.e., water without analytes, top) and the experimental group (5 μM Creatinine, bottom) with different concentrations of NaOH at the optimal concentration of Cit-AgNPs, respectively. The average grayscale change ($\Delta AG = AG_{Creatinine} - AG_{blank}$) of each TE response shown in (A) was provided in (B). Each error bar is the standard deviation of three repeated parallel experiments. The results showed that the largest ΔAG value was obtained from 600 mM NaOH. Therefore, the concentration of 600 mM NaOH was chosen as the optimal NaOH concentration for the next experiments.

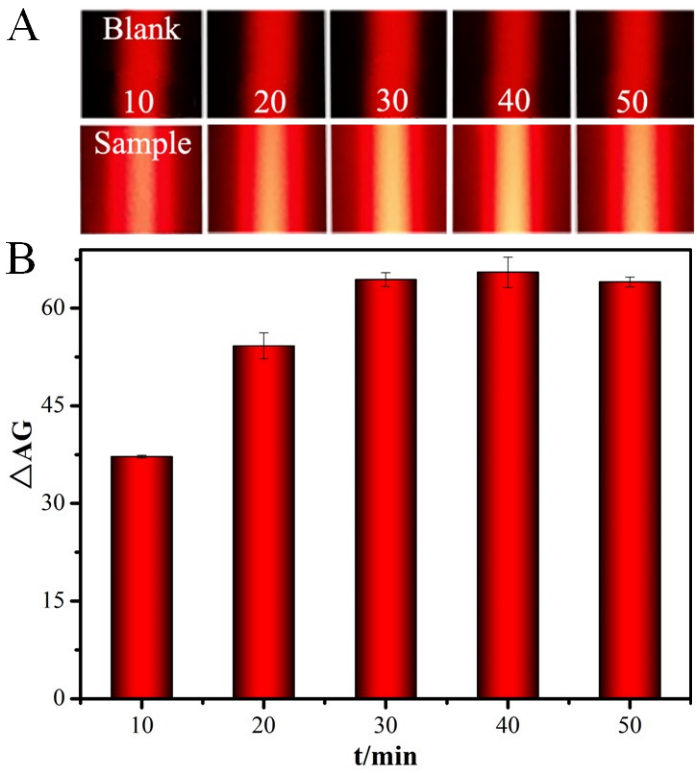

Fig. S4. (A) TE images obtained by mixing the blank group (i.e., water without analytes, top) and the experimental group (5 μM Creatinine, bottom) with different time of incubation time of samples with Cit-AgNPs, respectively. The average grayscale change ($\Delta AG = AG_{Creatinine} - AG_{blank}$) of each TE response shown in (A) was provided in (B). Each error bar is the standard deviation of three repeated parallel experiments. The results showed that the ΔAG value reached a maximum when the times reached 30 min. Therefore, 30 min was chosen as the optimal condition for the next experiments.

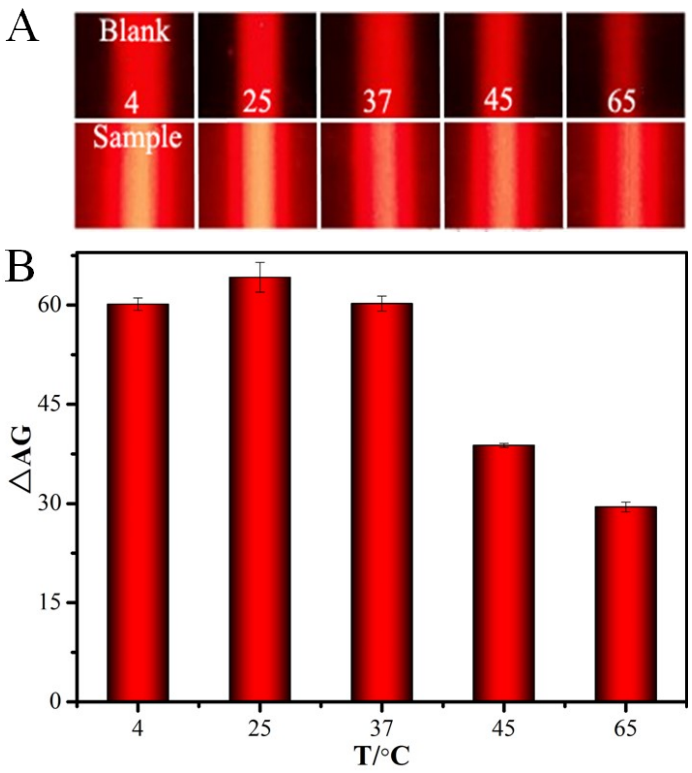

Fig. S5 (A) TE results obtained from the assays of blank samples (buffer without the analyte) and 5 μM Cre at different temperatures for the incubation of samples and AgNPs. The average grayscale change ($\Delta AG = AG_{Creatinine} - AG_{blank}$) of each TE response shown in (A) was provided in (B). Each error bar is the standard deviation of three repeated parallel experiments. The results showed that the largest ΔAG values were obtained with 25 °C (room temperature). Therefore, 25 °C was chosen as the optimal incubation temperature condition for the next experiments.

Table S1 Comparison of the present method with some previously reported methods employed in the detection of creatinine.

Probe	Signalling method	Quantifying method	LOD[a] (μM)	Sensitivity[b]	Portability	Ref.
Cyclodextrin-modified electrodes	Electrochemical method	Potentiometry	50	-	No	[2]
Miniaturized enzyme electrodes	Electrochemical method	Current	25	13.9 signal/M	No	[3]
AuNPs@MoS_2-NPs@GO	LSPR[c]	LSPR[c] spercrum	128.4	0.0025 signal/μM	No	[4]
AuNPs	SPR[d]	UV-vis spectrum	80	-	No	[5]
AuNPs	SPR[d]	UV-vis spectrum	121	0.2376 signal/μM	No	[6]
AuNPs	Fluorescence	fluorescence spectrum	2.87	-	No	[7]
AgNPs/PVP	SPR[d]	UV-vis spectrum	2.12	-0.3207 signal/μM	No	[8]
single-layer AgNP film	Raman scattering	SERS[e] spectrum	5	963.63 signal/μM	No	[9]
Nano-Ag/Au@Au film	Raman scattering	SERS[e] spectrum	5	0.27 signal/μM	No	[10]
AgNPs	TE	Smartphone imaging	0.055	580.8227 signal/nM	Yes	This work

[a]LOD, limit of detection;

[b]Sensitivity, the slope of its corresponding regression equation;

[c]LSPR, localized surface plasmon resonance;

[d]SPR, surface plasmon resonance;

[e]SERS, surface-enhanced Raman spectroscopy.

References:

1. Banerji, B.; Pramanik, S. K., Binding studies of creatinine and urea on iron-nanoparticle. *Springerplus*, 2015, **4**, 708.
2. Naresh Kumar, T.; Ananthi, A.; Mathiyarasu, J.; Joseph, J.; Lakshminarasimha Phani, K.; Yegnaraman, V., Enzymeless creatinine estimation using poly(3,4-ethylenedioxythiophene) -β-cyclodextrin. *Journal of Electroanalytical Chemistry*, 2011, **661** (2), 303-308.
3. Marcel B. Mgd'irag Ionel C. Popescu ', S. U., Richard P. Buck Microfabricated amperometric creatine and creatinine biosensors. *Analytica Chimica Acta*, 1996, **319**, 335-345.
4. Li, M.; Singh, R.; Marques, C.; Zhang, B.; Kumar, S., 2D material assisted SMF-MCF-MMF-SMF based LSPR sensor for creatinine detection. *Opt Express*, 2021, **29** (23), 38150-38167.
5. He, Y.; Zhang, X.; Yu, H., Gold nanoparticles-based colorimetric and visual creatinine assay. *Microchimica Acta*, 2015, **182** (11), 2037-2043.
6. Sittiwong, J.; Unob, F., Detection of urinary creatinine using gold nanoparticles after solid phase extraction. *Spectrochim Acta A Mol Biomol Spectrosc*, 2015, **138**, 381-386.
7. Chen, C. H.; Lin, M. S., A novel structural specific creatinine sensing scheme for the determination of the urine creatinine. *Biosens Bioelectron*, 2012, **31** (1), 90-94.
8. Narimani, R.; Azizi, M.; Esmaeili, M.; Rasta, S. H.; Khosroshahi, H. T., An optimal method for measuring biomarkers: colorimetric optical image processing for determination of creatinine concentration using silver nanoparticles. *3 Biotech*, 2020, **10** (10), 416.
9. Yang, F.; Wen, P.; Li, G.; Zhang, Z.; Ge, C.; Chen, L., High-performance surface-enhanced Raman spectroscopy chip integrated with a micro-optical system for the rapid detection of creatinine in serum. *Biomed Opt Express*, 2021, **12** (8), 4795-4806.

10. Wen, P.; Li Chen, F. Y. C. G., Shunbo Li,Yi Xu, Self-assembled nano-AgAu@Au film composite SERS substrates show high uniformity and high enhancement factor for creatinine detection. *Nanotechnology*, 2021, **32** (2021), 395502.